Accepted Manuscript

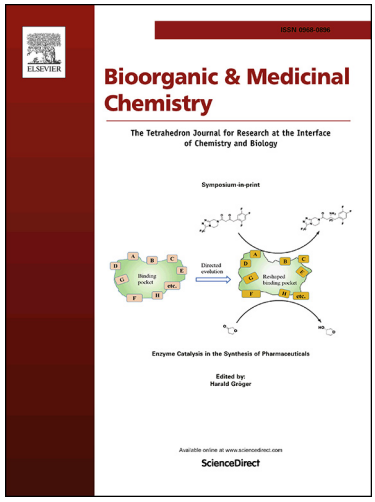

Synthesis and characterization of hydrogen peroxide activated estrogen receptor beta ligands

Hyejin Park, Joseph D. McEachon II, Julie A. Pollock

PII: S0968-0896(18)32079-0
DOI: https://doi.org/10.1016/j.bmc.2019.04.003
Reference: BMC 14857

To appear in: *Bioorganic & Medicinal Chemistry*

Received Date: 11 December 2018
Revised Date: 18 March 2019
Accepted Date: 2 April 2019

Please cite this article as: Park, H., McEachon, J.D. II, Pollock, J.A., Synthesis and characterization of hydrogen peroxide activated estrogen receptor beta ligands, *Bioorganic & Medicinal Chemistry* (2019), doi: https://doi.org/10.1016/j.bmc.2019.04.003

Graphical Abstract

To create your abstract, type over the instructions in the template box below.
Fonts or abstract dimensions should not be changed or altered.

Synthesis and characterization of hydrogen peroxide activated estrogen receptor beta ligands

Leave this area blank for abstract info.

Hyejin Park, Joseph D. McEachon II, and Julie A. Pollock
Department of Chemistry, University of Richmond, 138 UR Drive, Richmond, VA 23173, USA

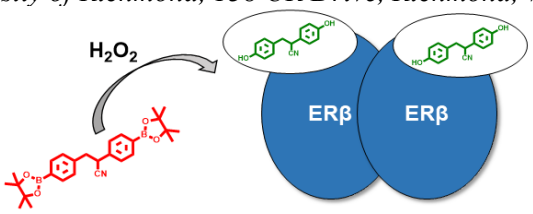

Bioorganic & Medicinal Chemistry
journal homepage: www.elsevier.com

Synthesis and characterization of hydrogen peroxide activated estrogen receptor beta ligands

Hyejin Park, Joseph D. McEachon II, and Julie A. Pollock*

Department of Chemistry, University of Richmond, 138 UR Drive, Richmond, VA 23173, USA

ARTICLE INFO

Article history:
Received
Received in revised form
Accepted
Available online

Keywords:
Estrogen
Pro-drug
Estrogen receptor beta
Boronic acid pinacol ester
Hydrogen peroxide

ABSTRACT

The development and evaluation of selective estrogen receptor modulators (SERMs) is of interest because of the complex and significant role of estrogen receptors in normal tissues as well as disease states. In neurodegenerative disorders such as Alzheimer's disease and multiple sclerosis, estrogen receptor beta (ERβ) seems to provide a protective anti-inflammatory response. Due to the increase in reactive oxygen species (ROS) in these diseases, we have masked ERβ ligands, including diarylproprionitrile (DPN), as boronate esters that release the active estrogen in the presence of H_2O_2. Here we demonstrate their synthesis, decreased binding affinities, kinetics of release, and selectivity toward ROS. The most promising ligand can be unmasked in the presence of pathological H_2O_2 to modulate ERβ transcription in cells.

1. Introduction

In response to sensing infections and injury, the immune system initiates and amplifies expression of innate immunity genes and adaptive immune responses. This burst of inflammatory activity is important in surmounting the infection or repairing the injury, but it is intended to be a local and time-limited event that normally undergoes abatement. When resolution is limited or incomplete, inflammation becomes chronic. Within the central nervous system, this deregulation of inflammation can be linked to neurodegenerative diseases such as Alzheimer's disease, multiple sclerosis, and Parkinson's disease[1]. Within these inflammatory environments, there is typically an overproduction of reactive oxygen species (ROS) including hydrogen peroxide (H_2O_2), hydroxyl radical (·OH), superoxide ($O_2^{-\cdot}$), and nitric oxide (NO)[2].

The role of estrogens and their receptors – estrogen receptor alpha (ERα) and estrogen receptor beta (ERβ) – in biology, including inflammation, is complex.Estrogen appears to provide neuroprotection through its actions as a potent anti-oxidant, anti-apoptotic, and anti-inflammatory agent[3]. Therefore, we set out to mask ER ligands for release in the presence of ROS. Boronate esters have been used extensively for the protection or masking of phenols due to their rapid and quantitative release in aqueous H_2O_2[4]. They have been developed for the selective detection and imaging of H_2O_2[5] and since been utilized as pro-drugs of matrix metalloproteinases[6], masked chelators of metal ions[7,8], selectively activatable DNA cross-linking agents[9,10], cytotoxic agents[11], and pro-drugs of histone deacetylase inhibitors[12].

The idea of boron-based pro-estrogens has been utilized before; in previous studies, the selective estrogen receptor modulators (SERMs) tamoxifen and endoxifen have been masked as boronate esters[13-15]. Tamoxifen and endoxifen both target ERα as therapies for breast cancer. The previous work focused mostly on the cellular consequences of these boronate ester SERMs observing similar or enhanced effects to the unmodified anti-estrogens in breast cancer cells. They were able to observe the presence of the SERMs after incubation of the boronate esters with MCF7 or T47D cells, presumably due to increased levels of ROS[13,15]. In addition, they showed increased bioavailability and drug accumulation at tumor sites within mouse xenograft models[16].

Due to the successes of tamoxifen and endoxifen boronate esters, we set out to mask alternative estrogens. In particular, we focused on the potent and selective ERβ agonist diarylpropionitrile (DPN, **Fig. 1a**)[16,17]. ERβ selective ligands, such as DPN, have shown significant promise in exhibiting neuroprotective effects in a number of neurological diseases[18-24]. In addition, molecules that activate ERβ repress transcription of proinflammatory genes; specifically, DPN has been shown to be effective in a model of inflammation following lung injury[25]. Due to the increased levels of ROS and pathological oxidative stress within neurodegenerative disorders and inflammatory diseases, we hypothesize that appending a boronate ester to the ERβ ligand will allow for consumption H_2O_2 and simultaneous release of the active ligand achieving dual results. In addition, the masking of the active phenol would allow for selective release of the estrogen in the presence of H_2O_2, providing site-selective modulation of ER. Herein, we report the synthesis of boronic

*Corresponding author. Tel.: +1-804-484-1578; fax: +1-804-289-8233; email: jpollock@richmond.edu

acid pinacol ester pro-estrogens of endogenous estrogens and the ERβ-selective agonist DPN. The boronate esters have decreased affinity for both ERα and ERβ and are converted into the active phenol in the presence of H_2O_2 *in vitro* and in cells.

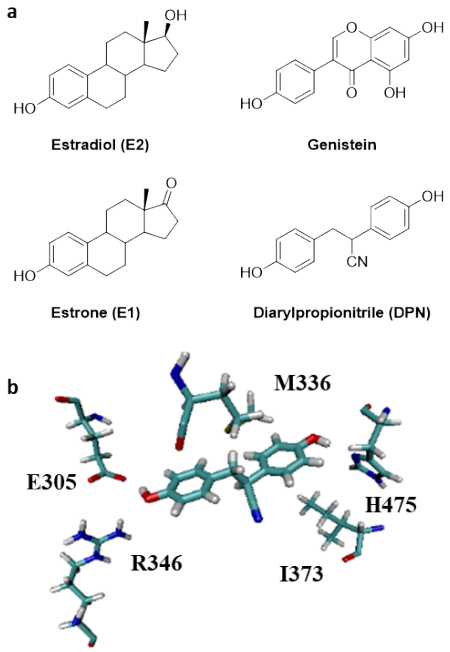

Figure 1. a) Structures of endogenous ER ligands, E2 and E1, and ERβ-selective agonists, genistein and DPN. b) DPN docked into the binding pocket of ERβ ligand binding domain (LBD). Only key residues are shown.

2. Results and discussion

2.1. Design of masked estrogens

It is well established in ER literature that the presence of a phenol is preferred for receptor binding (see reviews[26-28]). Indeed, endogenous estrogens such as estradiol (E2) and estrone (E1) as well as phytoestrogens such as genistein and the synthetic ERβ selective ligand DPN contain A-ring phenols (**Fig. 1a**). Crystal structures of estradiol[29] and genistein[30] bound into the ligand binding domain (LBD) of ERβ indicate that the A-ring phenol of the ligands forms hydrogen bonds with glutamate 305 and arginine 346 (**Fig. S1**). When we performed docking studies of DPN into ERβ LBD (PDB: 1X7J), there was no surprise that the best scoring hit placed the A-ring of DPN in the same position (**Fig. 1b**). Therefore, we set out to block the phenols on DPN as well as estradiol. Although a variety of boronate esters have been used as H_2O_2 activatable groups, we selected the boronic acid pinacol ester for the large size that could cause steric clashes to inhibit interaction with the ER binding pocket.

2.2. Chemistry

Our initial efforts focused on masking the endogenous steroidal estrogen, 17β-estradiol as a boronic acid pinacol ester on the A-ring of the steroid as a proof of principle. A previous study had examined boronated estrone derivatives and their oxidation to estrone in the presence of H_2O_2[31]. However, since our route to the boronated estradiol (**3**) required synthesis of the corresponding estrone (**2**), we evaluated both protected endogenous estrogens. These compounds were obtained through a straightforward modification of estrone (**Scheme 1**). The phenol of estrone was activated as the corresponding triflate (**1**) and palladium-mediated cross-coupling allowed installation of the boronic acid pinacol ester (**2**) in good yield. Reduction of the ketone resulted in the corresponding boronic acid pinacol ester 17β-estradiol (**3**) in good yield.

Next, we turned to the non-steroidal ERβ selective agonist, DPN. Since DPN contains two phenolic groups, we synthesized three derivatives with either one or both phenols masked as boronic acid pinacol esters. We generated DPN following literature precedent and the boronate ester DPNs (**6a-6c**) with a modified protocol (**Scheme 2**)[16]. First, compounds **4a-4c** were prepared through a base-mediated aldol condensation of the appropriate arylaldehydes and phenylacetonitriles in excellent yields. The alkenes were reduced using sodium borohydride to generate compounds **5a-5c** in moderate to good yields. Removal of the methyl protecting groups on **5a** and **5b** was successful using aluminum chloride and 1-dodecanethiol. Finally, palladium-mediated cross-coupling of the bromide with bis(pinacolato)diboron allowed the installation of the boronic acid pinacol esters (**6a-6c**) albeit with poor yields.

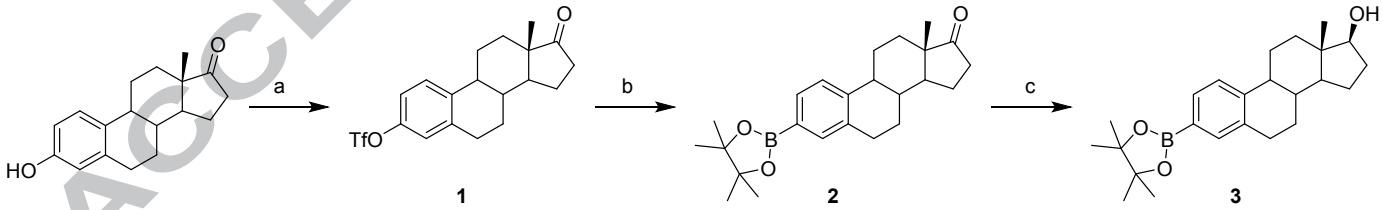

Scheme 1. Synthesis of boronic acid pinacol ester estrone (**2**) and estradiol (**3**). Reagents and Conditions (a) trifluoromethane sulfonic anhydride, 2,6-lutidine, dimethylaminopyridine, CH_2Cl_2, 0 °C, 1 h (70 %); (b) pinacolborane, $Pd(dppf)Cl_2$, triethylamine, dioxane, 100 °C, 18 h (82 %); (c) $NaBH_4$, methanol/tetrahydrofuran, 0 °C (78 %).

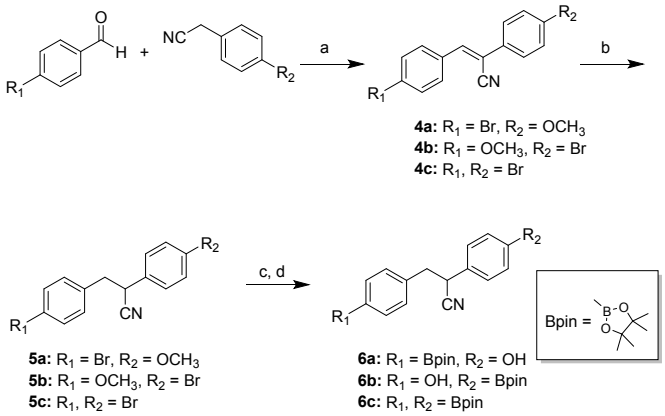

Scheme 2. Synthesis of boronic acid pinacol ester DPNs (**6a-6c**). Reagents and Conditions (a) 40% KOH, EtOH, rt. 1.5 h (**4a**, 95%; **4b**, 100%; **4c**, 100%) (b) $NaBH_4$, EtOH, 70 °C, 18 h (**5a**, 83%; **5b**, 82%; **5c**, 34%) (c) $AlCl_3$, 1-dodecanethiol, CH_2Cl_2 (34%) (d) bis(pinacolato)diboron, KOAc, $Pd(dppf)Cl_2$, 80 °C, 18 h (**6a**, 34%; **6b**, 35%; **6c**, 17%).

2.3. Estrogen receptor binding affinity

The boronate ester pro-estrogens were evaluated in competitive fluorescence polarization binding assays to

determine their affinities for full length ERα and ERβ (**Fig. S2**). Binding affinities shown in **Table 1** are expressed as relative binding affinity (RBA) values (estradiol = 100%) and were calculated using previously described methods[32]. The binding affinity of the phenolic estradiol, estrone, and DPN matched previous literature[16,33]. As expected, the binding affinities decreased, although in most cases moderately, when the phenols were replaced with boronic acid pinacol esters. For both ERα and ERβ, the RBA of **2** was approximately 6-fold less than estrone and the RBA of **3** was approximately 3-fold less than estradiol. As noted above, DPN is selective for ERβ over ERα; however, we observed a decrease in binding affinity for **6a-6c** for both receptors. For ERα, **6a** and **6b** had 4.5- and 6-fold decreased affinity while **6c** did not compete productively. For ERβ, the binding affinity of **6a** and **6b** decreased approximately 5-fold while **6c** decreased 20-fold in comparison to DPN. We were surprised that placement of the boronic ester in either of the R_1 (**6a**) or R_2 (**6b**) positions essentially resulted in the same decreased binding affinity; from previous studies of DPN and derivatives as well as our docking results (**Fig. 1b**), we expected replacement of the A-ring phenol (**6a**) to have more of an effect on binding[16]. The moderate decrease in binding affinities for compounds **6a** and **6b** is most likely because they still contain one free phenol and are capable of fitting into the flexible binding pocket of ERβ. Not surprisingly, however, was the fact that replacement of both phenols resulted in the poorest binder, **6c**.

Table 1. Estrogen receptor relative binding affinities

Compound	RBA[a]	
	ERα	**ERβ**
Estrone (E1)	12.8 ± 4.0	14.5 ± 11.6
Estradiol (E2)	100	100
DPN	0.392 ± 0.062	7.7 ± 4.4
2	2.2 ± 1.1	2.5 ± 1.4
3	33.0 ± 12.5	34.0 ± 10.1
6a	0.087 ± 0.023	1.58 ± 0.36
6b	0.063 ± 0.024	1.68 ± 1.22
6c	< 0.001	0.39 ± 0.26

[a]RBA = relative binding affinity, where estradiol = 100%. Data are presented as mean ± standard deviation of three replicates for E1, **2**, **3**, DPN, **6a-6c** and six replicates for E2.

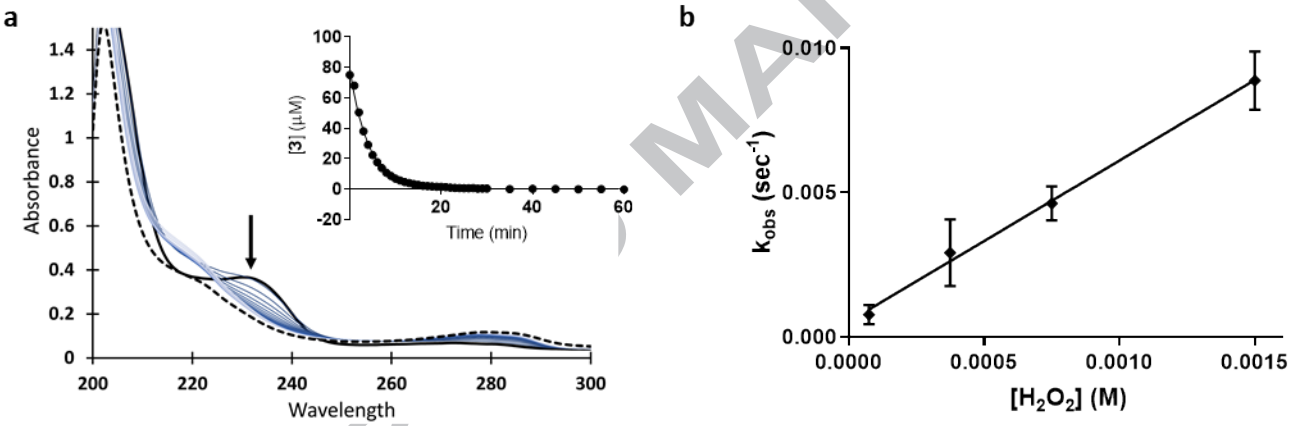

Figure 1. Kinetics of reaction of **3** with H_2O_2. a) Absorbance spectra of **3** (75 μM) with 10-fold H_2O_2 (750 μM) over 4 hours in PBS at 37 °C. Blue decreased in shade over time; scans taken every minute for the first 30 minutes, then every 5 minutes until 1 hour and every hour until 4 hours. **3** is black; E2 is dashed black. inset: data fit to a pseudo-first order model for reactant consumption during the reaction. b) Linear fit of k_{obs} and [H_2O_2]for conversion of **3** to E2 gives the second-order rate constant. Data presented as mean ± standard deviation of three replicates.

2.4. Kinetics of H_2O_2-mediated conversion to phenol

We first investigated the boronate ester estradiol **3** as our model system to evaluate H_2O_2-activation. The reaction was monitored in real time by UV spectroscopy in PBS (pH 7.4) at 37 °C for four hours to mimic a biological environment (**Fig. 2**). As illustrated in **Figure 2a**, pro-estrogen **3** exhibits moderate absorbance at 235 nm while E2 does not. Upon addition of 10 equivalents of H_2O_2, the peak at 235 nm decreases overtime eventually producing an absorbance spectrum equal to that of E2. Kinetic analysis of the data collected under pseudo-first order conditions (**Fig. 2a, inset**) gave a second order rate constant of 5.57 ± 0.23 $M^{-1}sec^{-1}$ for disappearance of the starting material (**Fig. 2b**). The conversion of **3** to E2 was confirmed by GC-MS analysis of the reaction mixture after 30 minutes of incubation; the retention time moved from 15.7 min to 12.5 min and the masses corresponded to the expected compounds (**Fig. S4**). In addition, reaction of pro-estrogen **2** with H_2O_2, when monitored by UV spectroscopy and quantified by consumption of absorbance at 235 nm, produced E1 at a similar rate with a second order rate constant of 4.81 ± 0.86 $M^{-1}sec^{-1}$ (**Fig. S3**). It is important to note that incubation of **3** or **2** alone in PBS for 4 hours at 37 °C did not result in a change in the UV spectra (**Fig. S5a**).

Next, we examined the boronic acid pinacol ester masked DPN derivatives **6a-6c** in similar conditions. DPN exhibited a stronger absorbance at 275 nm than any of the boronate derivatives. Therefore, we monitored the conversion of each compound to DPN using UV spectroscopy in PBS (pH 7.4) at 37 °C for four hours (**Fig. 3**). Similar to the estrone and estradiol pro-estrogens, there was complete conversion in approximately 10 minutes after addition of 10 equivalents of H_2O_2 (**Fig. 3a-c**). Kinetic analysis of the data at various concentrations of peroxide revealed that the second order rate constants for appearance of the product DPN were fairly consistent for each derivative **6a-6c** with second order rate constants of 6.46 ± 1.01 $M^{-1}sec^{-1}$, 5.92 ± 0.57 $M^{-1}sec^{-1}$, and 5.14 ± 0.29 $M^{-1}sec^{-1}$, respectively (**Fig. S6, 3d**). Not surprisingly, **6c**, which contains two boronic acid

pinacol esters, was slightly slower than **6a** and **6b**. We were unable to uncouple the conversion of one pinacol boronate to the phenol from the other because there was not a differential wavelength to monitor; however, DPN was observed as the product at the end of the reaction time (**Fig. 3c**). As above, incubation of **6a-6c** in PBS for 4 hours at 37 °C did not result in changes in the UV spectra (**Fig. S5b**). The second order rate constants for the conversion of any of the boronate ester compounds here is consistent with previously presented systems[6,8].

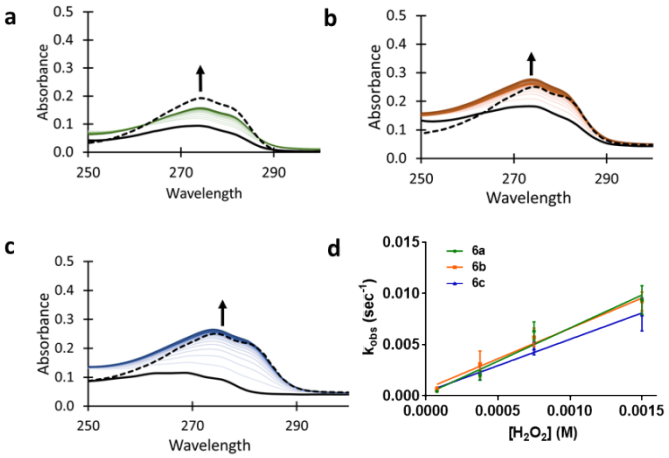

Figure 3. Kinetics of reaction of **6a-6c** with H_2O_2. a) Absorbance spectra of **6a** (75 µM) with 10-fold H_2O_2 (750 µM) over 4 hours in PBS at 37 °C. Green decreases in shade over time; scans taken every minute for the first 30 minutes, then every 5 minutes until 1 hour and every hour until 4 hours. **6a** is black; DPN is dashed black. b) Absorbance spectra of **6b** (75 µM) with 10-fold H_2O_2 (750 µM) over 4 hours in PBS at 37 °C. Orange decreases in shade over time; scans taken every minute for the first 30 minutes, then every 5 minutes until 1 hour and every hour until 4 hours.vv **6b** is black; DPN is dashed black. c) Absorbance spectra of **6c** (75 µM) with 10-fold H_2O_2 (750 µM) over 4 hours in PBS at 37 °C. Blue decreases in shade over time; scans taken every minute for the first 30 minutes, then every 5 minutes until 1 hour and every hour until 4 hours. **6c** is black; DPN is dashed black. d)) Linear fit of k_{obs} and [H_2O_2]for conversion of **6a** (green), **6b** (orange), and **6c** (blue) to DPN gives the second-order rate constant. Data presented as mean ± standard deviation of three replicates.

2.5. ROS Selectivity

Since H_2O_2 is not the only ROS in biological systems, we examined the reactivity of the boronate esters toward other ROS, including tert-butylhydroperoxide (TBHP), hypochlorite (OCl^-), nitric oxide (NO), hydroxyl radical (·OH), and superoxide ($O_2^{-\cdot}$). We chose to focus on the DPN pro-estrogens **6a-6c** because of the selectivity for ERβ and therapeutic implications in neuroinflammatory disorders. Due to background absorbance issues with the alternative ROS, we analyzed the end points of these reactions using HPLC (**Fig. 4a-c**). The retention time for DPN was 19 min while the retention time for **6a**, **6b**, and **6c** were 22 min, 23 min, and 28 min, respectively. As expected after 1 hour of exposure to 5-fold H_2O_2, all of the pro-estrogens were converted to DPN. Alternatively, incubation with 5-fold TBHP, NO, and hydroxyl radical did not convert **6a-6c** into DPN. In addition, there was approximately 22 % conversion of the boronate esters in the presence of 5-fold superoxide and 50-80 % consumption in the presence of 5-fold hypochlorite (**Fig. 4d**). We were able to observe small conversion of **6c** to **6a** and **6b** with both superoxide and hypochlorite, indicating oxidation of one boronate ester (**Fig. 4c**). There were approximately equal amounts of **6a** and **6b** in those cases indicating no selectivity for one boronate ester over the other. Some boronate ester peaks were observed to broaden or misshapen (most evident in **Fig. 4b** with NO trace) that we attribute to artifacts of the HPLC. When we examined the UV spectra recorded by the photodiode array, the spectra aligned well with **6b** across the full retention time, changing only in absorptivity and not shape; in addition, purity measurements by the photodiode array indicated that the purity threshold was met along the peak (**Fig. S7**). The DPN boronate esters showed less selectivity, specifically against OCl^-, in comparison to previous experimentation on the estrone boronate ester **2** that showed minimal reactivity in the presence of hypochlorite[23]. However, other groups have observed this phenomena indicating that hypochlorite is another promising ROS that can convert boronate esters into phenols[34,35].

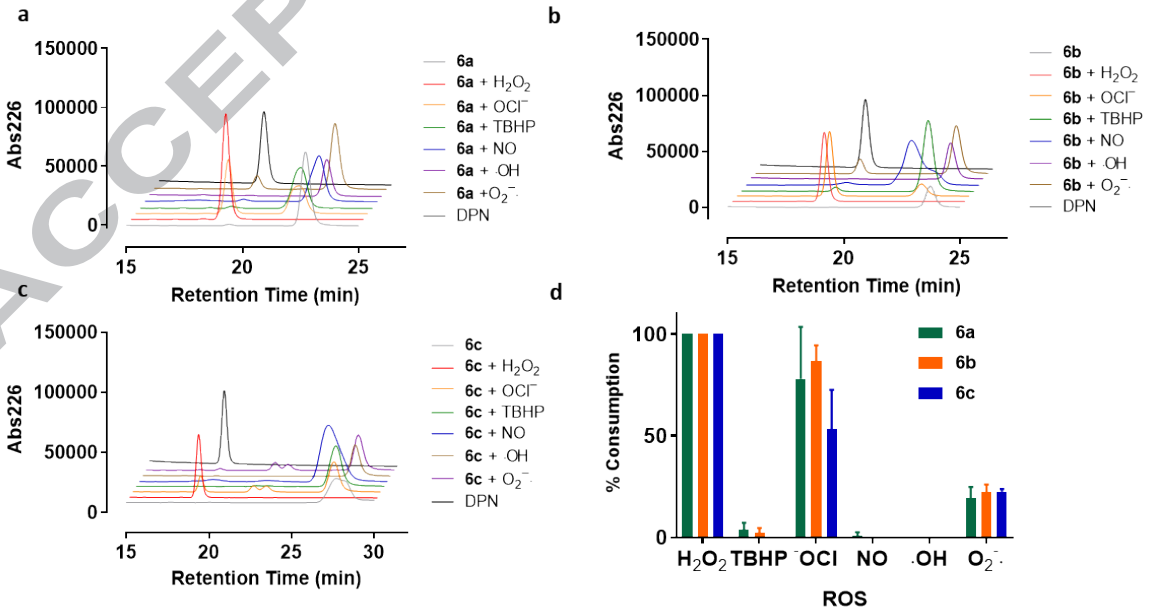

Figure 4. HPLC monitoring of reaction of **6a-6c** with various reactive oxygen species. a) Reaction of **6a** (150 µM, gray) with 5-fold of each ROS for 1 hour in PBS at 37 °C. b) Reaction of **6b** (150 µM, gray) with 5-fold of each ROS for 1 hour in PBS at 37 °C. c) Reaction of **6c** (150 µM, gray) with 5-fold of each ROS for 1 hour in PBS at 37 °C. Each line is representative of one replicate. d) Quantification of consumption of **6a-6c** (green, orange, blue, respectively) incubated for 1 hour with 5-fold of different reactive oxygen species (ROS). Data is presented as mean ± standard deviation of three replicates. NO was generated from NOC5, superoxide was generated from a xanthine oxidase reaction, and hydroxyl radical was generated from Fe^{2+} and H_2O_2. (See experimental for complete reaction conditions)

This lack of selectivity is not a downfall for compounds **6a-6c** because increased levels of the oxidant hypochlorite have also been linked to a variety of inflammatory diseases such as Alzheimer's disease[36]. Therefore, release of the active ERβ ligand in the presence of multiple ROS could allow for advantageous protective effects.

2.6. ERβ transcriptional activation

In order to probe the therapeutic potential of the boronate ester masked DPN ligands, we examined the ability to activate ERβ transcriptional activity in a cellular environment using a luciferase-based assay. We chose to focus on the most promising compound, **6c**, which was rapidly converted to DPN in the presence of excess H_2O_2 (**Fig. 3c**) but also resulted in the most detrimental effect on ER binding (**Table 1**). As seen in **Figure 5a**, E2 and DPN exhibited potencies (EC_{50} = 0.020 nM and 0.72 mM, respectively) consistent with literature as expected (EC_{50} = 0.030 mM and 0.89 nM, respectively)[16]. However, treatment of the cells for 24 hours with **6c** less potent (**Fig. 5b**, EC_{50} = 470 nM). As pathological levels of H_2O_2 in Alzheimer's disease models and other inflammatory disorders have been reported to be at least 100 μM[37-39], we added exogenous H_2O_2 at 50 μM and 100 μM to mimic the inflammatory environment. The potency of E2 and DPN did not change upon addition of H_2O_2; however, the transcriptional potency of **6c** increased (**Fig. 5b**, EC_{50} = 6.1 nM and 1.2 nM, respectively). At the highest concentration of H_2O_2 used, **6c** behaved most similarly to DPN, indicating that the active ligand was released in the cellular environment at these pathological levels.

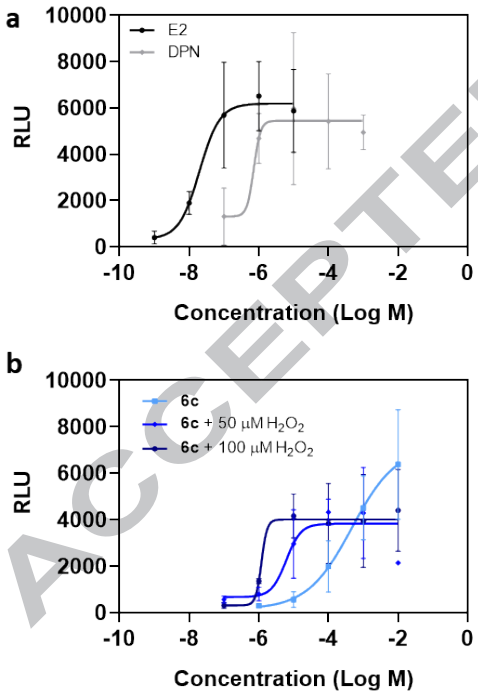

Figure 5. Transcriptional activation by ERβ in response to ligands after 24 hours treatment at the indicated concentrations. a) Control experiments with E2 and DPN. Values are given as mean ± standard deviation of four replicates. b) Experiments with **6c** without H_2O_2 (squares, n = 6), **6c** with 50 μM H_2O_2 (diamonds, n =4), and **6c** with 100 μM H_2O_2 (circles, n = 6). Values are given as mean ± standard deviation of replicates as indicated.

3. Conclusions

In summary, we have prepared several steroidal and non-steroidal boronate esters as pro-estrogens for the estrogen receptors. They are converted rapidly and completely to the phenolic estrogens when reacted with H_2O_2. In addition, the presence of the boronic acid pinacol ester decreases the binding affinity for both ERα and ERβ by 3-20 fold depending on the ligand. The ERβ-selective ligand DPN was masked as three different boronate esters **6a-6c**, which have similar functionality and reactivity *in vitro*. The integration of a ROS reactive group into a functional estrogen has implications in a variety of neurodegenerative and inflammatory diseases. The pro-estrogens **6a-6c** could have dual effects in absorbing H_2O_2 and releasing an ERβ-selective ligand with therapeutic potential. In particular, pro-estrogen **6c**, that masks both phenolic rings, exhibits increased selectivity for H_2O_2, and diminishes the binding affinity for the receptors most significantly. In addition, the ERβ agonist activity is masked by the boronate esters of **6c** in a cellular environment; however, when H_2O_2 is at a pathological level, the agonist activity is restored.

This work expands upon previous studies with boronate ester linked SERMs in breast cancer contexts illustrating together that the installation of a boronate ester is a promising pro-drug strategy for ER modulation. Due to the complexity of ER signaling, context specific estrogens (e.g. SERMs and subtype-selective ligands) are constantly being developed. The release of an active ER ligand in the presence of H_2O_2 provides an alternative approach to developing context specific estrogens or anti-estrogens.

4. Experimental

4.1. Synthesis

Reagents and solvents for synthesis were purchased from commercial sources and used without further purification. ^{1}H and ^{13}C NMR were recorded on a 500 MHz spectrometer or a 300 MHz spectrometer and are reported in ppm using solvent as an internal standard. Preparative column chromatography was performed on silica gel (230-400 mesh) and thin-layer chromatography (TLC) was carried out using pre-coated silica gel plates.

4.1.1. Synthesis of boronic ester estrone and estradiol

*4.1.1.1. Synthesis of triflate estrone (**1**)*

Dimethylaminopyridine (0.058 g, 0.45 mmol), 2,6-lutidine (0.46 mL, 3.48 mmol) and trifluoromethane sulfonic anhydride (0.35 mL, 2.23 mmol) were added to a solution of estrone (0.5 g, 1.85 mmol) in dichloromethane (15 mL). The reaction mixture was stirred at 0 °C for 1 h and was washed with 10 % HCl, 10 % $NaHCO_3$ and brine. The resulting solution was dried with Na_2SO_4 and concentrated under vacuum. The product was purified using silica gel column, eluted with dichloromethane/hexane (9:1) to obtain estrone triflate (**1**) as a white crystal (0.41 g, 56 %): ^{1}H NMR (300 MHz, $CDCl_3$) δ 7.33 (dd, *J* = 8.6, 1.0 Hz, 1 H), 7.07 – 6.96 (m, 2 H), 2.93 (dd, *J* = 8.7, 4.3 Hz, 2 H), 2.50 (dd, *J* = 18.2, 8.4 Hz, 1 H), 2.45 – 2.34 (m, 1 H), 2.29 (td, *J* = 10.5, 9.5, 3.7 Hz, 1 H), 2.22 – 1.89 (m, 4 H), 1.73 – 1.33 (m, 6 H), 0.91 (s, 3 H); ^{13}C NMR (75 MHz, $CDCl_3$) δ 220.2, 147.6, 140.3, 139.3, 127.2, 125.1, 121.2, 120.9, 118.3, 116.6, 112.4, 50.4, 47.8, 44.1, 37.8, 35.7, 31.5, 29.3, 26.1, 25.7, 21.5, 13.8.

*4.1.1.2. Synthesis of boronic ester estrone (**2**)*

To a mixture of **1** (0.5 g, 1.28 mmol) and $Pd(dppf)Cl_2$ (41.8 mg, 0.049 mmol) under nitrogen were added 1,4-dioxane (6.2 mL, 72.7 mmol), triethylamine (1 mL, 7.5 mmol) and pinacolborane (0.5 mL, 3.58 mmol). The reaction mixture was heated to 100 °C and stirred overnight. After cooling to room

temperature, the crude reaction mixture concentrated *in vacuo*, and purified with silica gel column using ethyl acetate/hexane (1:3) to afford boronic ester estrone (**2**) as a white solid (0.37 g, 76 %): ^{1}H NMR (300 MHz, $CDCl_3$) δ 7.70 – 7.53 (m, 2 H), 7.33 (d, *J* = 7.7 Hz, 1 H), 3.05 – 2.83 (m, 2 H), 2.61 – 2.40 (m, 2 H), 2.35 (td, *J* = 10.4, 4.2 Hz, 1 H), 2.27 – 1.89 (m, 5 H), 1.73 – 1.44 (m, 4 H), 1.36 (s, 12 H), 0.93 (d, *J* = 2.8 Hz, 3 H); ^{13}C NMR (75 MHz, $CDCl_3$) δ 220.7, 143.1, 135.8, 135.6, 132.2, 124.8, 83.7, 50.6, 48.0, 44.7, 38.1, 35.8, 31.6, 29.1, 26.5, 25.6, 24.8, 24.8, 21.6, 13.8. HRMS (ESI-TOF) exact mass calcd for $C_{24}H_{35}O_3BNa$ $[M+Na]^+$ 405.2576, found 405.2594.

*4.1.1.3. Synthesis of boronic ester estradiol (**3**)*

2 (0.35 mg, 0.92 mmol) was dissolved in a mixture of 1:1 v/v methanol/tetrahydrofuran (6 mL) and was cooled in an ice bath. Sodium borohydride (148 mg, 3.83 mmol) was added portion wise and stirred until the starting material was consumed as indicated by TLC analysis. Brine (20 mL) and excess water was added to the reaction mixture and extracted with dichlormethane (2 x 20 mL). The combined organic layers were washed with brine and dried with Na_2SO_4. The solution was concentrated under vacuum and purified using silica gel chromatography using CH_2Cl_2/hexane (9:1) to yield boronic ester estradiol (**3**) as a white solid (0.27 g, 78 %): ^{1}H NMR (300 MHz, $CDCl_3$) δ 7.61 – 7.55 (m, 2 H), 7.34 – 7.31 (m, 1 H), 3.77 – 3.71 (m, 1 H), 2.90 (dd, I = 8.7, 4.3 Hz, 2 H), 2.46 – 2.23 (m, 2 H), 2.23 – 2.05 (m, 1 H), 2.05 – 1.83 (m, 2 H), 1.86 – 1.63 (m, 1 H), 1.36 (s, 12 H), 0.81 (dd, *J* = 3.0, 0.6 Hz, 3 H); ^{13}C NMR (75 MHz, $CDCl_3$) δ 143.8, 136.1, 135.6, 132.0, 124.8, 83.2, 81.9, 50.3, 44.7, 43.2, 38.5, 36.8, 31.9, 30.6, 29.7, 29.7, 29.4, 29.3, 27.2, 26.0, 24.8, 24.8, 23.2, 22.7, 14.1, 11.0. HRMS (ESI-TOF) exact mass calcd for $C_{24}H_{33}O_3BNa$ $[M+Na]^+$ 403.2419, found 403.2413.

4.1.2. Synthesis of boronic ester DPNs

4.1.2.1. General procedure for arylacetonitrile/aldehyde condensation

A solution of 40% aqueous KOH (0.23 mL/mmol nitrile) was diluted with EtOH (0.46 mL/mmol nitrile) and was added to the solution of appropriate arylaldehyde (1.1 equiv.) and arylacetonitrile (1.0 equiv.) in EtOH (0.35 mL/mmol nitrile) at room temperature, which resulted in immediate formation of white precipitate. The reaction mixture was stirred for 1.5 hours and the precipitate was collected through vacuum filtration. The residue was washed with water and cold EtOH.

*4.1.2.1.1. Compound **4a***

Prepared from 4-bromobenzaldehyde (406 mg, 2.2 mmol) and 4-methoxyphenylacetonitrile (0.272 mL, 2.0 mmol) to produce yellow solid (0.592 g, 95 %): ^{1}H NMR (300 MHz, $CDCl_3$) δ 7.71 (d, *J* = 8.5 Hz, 2 H), 7.58 (dd, *J* = 8.7, 8.0 Hz, 4 H), 7.33 (s, 1 H), 6.95 (d, *J* = 8.9 Hz, 2 H), 3.85 (s, 3 H); ^{13}C NMR (75 MHz, $CDCl_3$) δ 160.7, 138.5, 132.9, 132.2, 130.5, 127.4, 126.7, 124.4, 117.9, 114.6, 112.1, 55.5.

*4.1.2.1.2. Compound **4b***

Prepared from 4-methoxybenzaldehyde (0.260 mL, 2.2 mmol) and 4-bromophenylacetonitrile (0.392 g, 2.0 mmol) to produce yellow solid (0.653 g, 100 %): ^{1}H NMR (300 MHz, $CDCl_3$) δ 7.88 (d, *J* = 8.7 Hz, 2 H), 7.59 – 7.48 (m, 4 H), 7.44 (s, 1 H), 6.98 (d, *J* = 8.9 Hz, 2 H), 3.87 (s, 3 H); ^{13}C NMR (75 MHz, $CDCl_3$) δ 161.8, 142.3, 134.0, 132.3, 131.4, 127.4, 126.4, 123.0, 118.3, 114.6, 107.6, 55.6.

*4.1.2.1.3. Compound **4c***

Prepared from 4-bromobenzaldehyde (406 mg, 2.2 mmol) and 4-bromophenylacetonitrile (389 mg, 2.0 mmol) to produce yellow solid (0.726 g, 100 %): ^{1}H NMR (300 MHz, $CDCl_3$) δ 7.75 (d, *J* = 8.5 Hz, 2 H), 7.63 – 7.56 (m, 4 H), 7.54 (s, 2 H), 7.44 (s, 1 H); ^{13}C NMR (75 MHz, $CDCl_3$) δ 141.0, 133.1, 132.3, 130.7, 127.5, 125.2, 123.8, 117.3, 111.4.

4.1.2.2. General procedure for reduction

$NaBH_4$ (1.0 equiv.) was added slowly to a solution of diarylpropionitrile (1.0 equiv.) in EtOH and pyridine under N_2 atmosphere. The reaction was stirred at 70 °C overnight, then cooled to room temperature and quenched with water. The reaction mixture was diluted with 100 mL H_2O and acidified with 6 M HCl. The organic layers were extracted with ether (3 x 50 mL), washed with brine and water, dried with Na_2SO_4, and concentrated *in vacuo*.

*4.1.2.2.1. Compound **5a***

Prepared as above with $NaBH_4$ (43 mg, 1.3 mmol) and **4a** (0.400 g, 1.3 mmol) in EtOH (4 mL) and pyridine (1 mL) to yield white solid (0.335 g, 83 %): ^{1}H NMR (300 MHz, $CDCl_3$) δ 7.40 (d, *J* = 8.4 Hz, 2 H), 7.14 (d, *J* = 8.8 Hz, 2 H), 6.98 (d, *J* = 8.3 Hz, 2 H), 6.87 (d, *J* = 8.7 Hz, 2 H), 3.96 (s, 1 H), 3.80 (s, 3 H), 3.08 (dd, *J* = 7.2, 4.7 Hz, 2 H); ^{13}C NMR (75 MHz, $CDCl_3$) δ 159.5, 135.3, 131.7, 131.0, 128.6, 126.7, 121.4, 120.4, 114.5, 55.4, 41.5, 38.6.

*4.1.2.2.2. Compound **5b***

Prepared as above with $NaBH_4$ (60.4 mg, 1.6 mmol) and **4b** (0.500 g, 1.6 mmol) in EtOH (5 mL) and pyridine (1 mL) to yield white solid (0.414 g, 82 %): ^{1}H NMR (300 MHz, $CDCl_3$) δ 7.47 (d, *J* = 8.4 Hz, 2 H), 7.10 (d, *J* = 8.4 Hz, 2 H), 7.01 (d, *J* = 8.6 Hz, 2 H), 6.82 (d, *J* = 8.6 Hz, 2 H), 3.93 (dd, *J* = 7.7, 6.6 Hz, 1 H), 3.79 (s, 3 H), 3.09 (dd, *J* = 8.9, 7.1 Hz, 2 H); ^{13}C NMR (75 MHz, $CDCl_3$) δ 159.0, 134.2, 132.1, 130.3, 129.2, 127.8, 122.2, 120.0, 114.01, 55.2, 41.1, 39.4.

*4.1.2.2.3. Compound **5c***

Prepared as above with $NaBH_4$ (53 mg, 1.4 mmol) and **4c** (0.500 g, 1.4 mmol) in EtOH (5 mL) and pyridine (1 mL) to yield white solid (0.171 g, 34 %): ^{1}H NMR (300 MHz, $CDCl_3$) δ 7.48 (d, *J* = 8.5 Hz, 2 H), 7.41 (d, *J* = 8.4 Hz, 2 H), 7.09 (d, *J* = 8.4 Hz, 2 H), 6.96 (d, *J* = 8.4 Hz, 2 H), 3.96 (t, *J* = 7.1 Hz, 1 H), 3.09 (dd, *J* = 7.2, 5.1 Hz, 2 H); ^{13}C NMR (75 MHz, $CDCl_3$) δ 134.6, 133.7, 132.3, 131.8, 131.0, 129.2, 122.5, 121.7, 119.6, 41.2, 38.9.

4.1.2.3. General deprotection and coupling methods

$AlCl_3$ (5 equiv.) and dodecanethiol (2 equiv.) were added to CH_2Cl_2 (2 mL) and cooled to 0 °C. Methyl ether (1 equiv.) in CH_2Cl_2 (1mL) was added to the $AlCl_3$/thiol solution. The mixture was allowed to warm up to room temperature and stirred overnight. The reaction mixture was then poured into ice water (50 mL) and the product was extracted with EtOAc (3 x 20 mL). The organic layers were combined and washed with water and brine. The organic layer was dried over Na_2SO_4 and concentrated under reduced pressure to yield crude product, which was purified by silica gel column chromatography using 1:5 EtOAc/hexane.

To a mixture of bis(pinacolato)diboron (1.1 equiv.), KOAc (3 equiv.) and $Pd(dppf)Cl_2$ (0.03 equiv.) in dioxane was added a solution of bromide (1 equiv.) in dioxane under N_2 atmosphere. The mixture was stirred at 80 °C overnight and the completion of the reaction was confirmed by TLC. The volatiles from the reaction mixture were removed under reduced pressure. The

residue was diluted with ethyl acetate (10 mL) and washed with water. The organic layers were combined, washed with brine, and dried over Na_2SO_4. The crude product was concentrated under reduced pressure and purified by silica gel column chromatography using 1:3 EtOAc/hexane.

*4.1.2.3.1. Compound **6a***

Prepared from **5a** (0.200 g, 0.64 mmol), $AlCl_3$ (0.423 g, 3.2 mmol) and dodecanethiol (0.30 mL, 1.3 mmol) according to the procedure above. After purification, the intermediate compound **a** was obtained as a white solid (0.066 g, 34 %): ^{1}H NMR (300 MHz, Acetone-d_6) δ 8.47 (s, 1 H), 7.46 (d, *J* = 8.3 Hz, 2 H), 7.26 – 7.12 (m, 4 H), 6.85 (d, *J* = 8.5 Hz, 2 H), 4.26 (t, *J* = 7.5 Hz, 1 H), 3.17 (d, *J* = 7.5 Hz, 2 H); ^{13}C NMR (75 MHz, Acetone-d_6) δ 206.2, 158.1, 137.5, 132.3, 132.2, 129.7, 127.4, 121.4, 121.4, 116.6, 41.6, 38.6. Prepared from intermediate compound **a** (93.5 mg, 0.31 mmol), bis(pinacolato)diboron (86.6 mg, 0.34 mmol), KOAc (88.2 mg, 0.93 mmol), Pd(dppf)Cl_2 (6.8 mg, 0.009 mmol) in dioxane (1.6 mL) as described above to afford compound **6a** (0.0364 g, 34 %): ^{1}H NMR (300 MHz, Acetone-d6) δ 8.42 (s, 1 H), 7.68 (d, *J* = 8.1 Hz, 2 H), 7.27 (d, *J* = 8.0 Hz, 2 H), 7.22 (d, *J* = 8.6 Hz, 2 H), 6.85 (d, *J* = 8.6 Hz, 2 H), 4.28 (t, *J* = 7.6 Hz, 1 H), 3.20 (d, *J* = 7.7 Hz, 2 H), 1.33 (s, 12 H); ^{13}C NMR (75 MHz, Acetone-d6) δ 206.1, 158.1, 141.5, 135.6, 132.4, 129.6, 127.7, 121.5, 116.6, 84.5, 42.6, 38.8, 25.2. HRMS (ESI-TOF) exact mass calcd for $C_{21}H_{24}NO_3BNa$ $[M+Na]^+$ 372.1745, found 372.1746.

*4.1.2.3.2. Compound **6b***

Prepared from **5c** (0.150 g, 0.48 mmol), $AlCl_3$ (0.314 g, 2.4 mmol) and dodecanethiol (0.29 mL, 1.2 mmol) according to the procedure above. After purification the intermediate compound **b** was obtained as white solid (0.049 g, 34 %): ^{1}H NMR (300 MHz, Acetone-d_6) δ 8.24 (s, 1 H), 7.56 (d, *J* = 8.5 Hz, 2 H), 7.32 (d, *J* = 8.4 Hz, 2 H), 7.06 (d, *J* = 8.5 Hz, 2 H), 6.77 (d, *J* = 8.5 Hz, 2 H), 4.31 (t, *J* = 7.5 Hz, 1 H), 3.12 (d, *J* = 7.4 Hz, 2 H); ^{13}C NMR (75 MHz, Acetone-d_6) δ 206.0, 132.7, 132.1, 131.3, 131.1, 130.9, 130.6, 115.8, 32.6, 23.3, 14.3. Prepared from the intermediate compound **b** (64 mg, 0.21 mmol), bis(pinacolato)diboron (60 mg, 0.23 mmol), KOAc (60.5 mg, 0.63 mmol) and Pd(dppf)Cl_2 (4.7 mg, 0.006 mmol) in dioxane (1.1 mL) as described above to afford compound **6b** (0.0256 g, 35 %): ^{1}H NMR (300 MHz, Acetone-d6) δ 8.19 (s, 1 H), 7.76 (d, *J* = 8.2 Hz, 2 H), 7.40 (d, *J* = 8.1 Hz, 2 H), 7.08 (d, *J* = 8.5 Hz, 2 H), 6.76 (d, *J* = 8.6 Hz, 2 H), 4.32 (t, *J* = 7.5 Hz, 1 H), 3.13 (d, *J* = 7.5 Hz, 2 H), 1.34 (s, 12 H); ^{13}C NMR (75 MHz, Acetone-d6) δ 206.1, 157.5, 140.3, 136.0, 131.3, 128.6, 127.9, 121.2, 116.1, 84.7, 41.6, 40.3, 25.2. HRMS (ESI-TOF) exact mass calcd for $C_{21}H_{24}NO_3BNa$ $[M+Na]^+$ 372.1745, found 372.1723.

*4.1.2.3.3. Compound **6c***

Prepared from **5c** (70 mg, 0.19 mmol), bis(pinacolato)diboron (108 mg, 0.42 mmol), KOAc (55 mg, 0.58 mmol) and Pd(dppf)Cl_2 (4.7 mg, 0.006 mmol) in dioxane (1.1 mL) according to the procedure above to afford compound **6c** (0.0145 g, 17 %): ^{1}H NMR (300 MHz, $CDCl_3$) δ 7.78 (d, *J* = 8.1 Hz, 2 H), 7.73 (d, *J* = 8.0 Hz, 2 H), 7.25 (d, *J* = 7.7 Hz, 2 H), 7.12 (d, *J* = 8.0 Hz, 2 H), 4.01 (dd, *J* = 7.9, 6.7 Hz, 1 H), 3.17 (dd, *J* = 10.3, 7.4 Hz, 2 H), 1.35 (s, 12 H), 1.34 (s, 12 H); ^{13}C NMR (75 MHz, $CDCl_3$) δ 139.2, 138.0, 135.4, 135.1, 128.6, 126.8, 120.0, 84.0, 83.8, 42.2, 39.7, 24.9. HRMS (ESI-TOF) exact mass calcd for $C_{27}H_{35}NO_4B_2Na$ $[M+Na]^+$ 482.2654, found 482.2663.

4.2. DPN docking

The X-ray structure of the ligand binding domain (LBD) of ERβ bound to genistein (PDB: 1X7J)[30] was used to dock DPN using Swissdock[40,41]. The analysis of the data and alignment of the structures was performed in VMD[42].

4.3. Estrogen receptor binding assays

The relative binding affinity (RBA) of the compounds were assessed using PolarScreen™ ERα and ERβ Competitor Assays, Green (Life Technologies). Briefly, stock solutions of the ligands (10 mM in DMSO) were serially diluted and added to premixed solutions of full length human recombinant ERα or ERβ with the fluormone tracer at concentrations suggested by the manufacturer in ES2 screening buffer (0.1 mg/mL acetylated BGG, 0.1 M potassium phosphate, pH 7.4, 0.02% sodium azide). The black 384-well plate was covered and incubated at room temperature for 2 hours and the fluorescence polarization was subsequently read using a SpectraMax i3 plate reader (ex. 485 nm, em. 535 nm). The polarization data was fit using GraphPad Prism 7 and IC_{50} values calculated. The RBA values were calculated from the IC_{50} values relative to that of estradiol for each replicate.

4.4. UV spectroscopy kinetic studies

Boronic ester solutions used for UV spectroscopy were prepared in 1 mL volumes at a final concentration of 75 μM in PBS with the indicated concentration of H_2O_2. Absorbance measurements were collected in a Cary 100 Bio UV-visible spectrophotometer. For the kinetic studies, absorbance at a range of 400-200 nm were measured once per minute for the first 30 minutes, every five minutes for 30–60 min, and then every half-hour for the remaining 3 hours for a simulated-first order boronic acid pinacol ester conversion. For determination of k_{obs}, absorbance values at 235 nm (for compound **2** or **3**) or 275 nm (for compounds **6a-6c**) were converted to boronic ester estrogen concentration at time, t, using the following equation:

$$[BEE]/[BEE]_0 = (A_t - A_{inf}) / (A_0 - A_{inf}) \quad (1)$$

where $[BEE]_0$ is the initial concentration of boronic ester estrogen prior to reaction with H_2O_2 and A_0 and A_{inf} are the absorbances measured respectively at reaction time t = 0, and t = infinity (full conversion to phenol). Concentration values were then entered into GraphPad Prism 7 and tested for mathematical fits. The model that provided the best fit for the data was an exponential decay model described by the equation:

$$[BEE] = [BEE]_0 * e^{kt} \quad (2)$$

where k is the observed rate constant k_{obs}.

4.5. Gas Chromatography-Mass Spectrometry (GCMS) analysis

Solutions of **3** used for GCMS were prepared in 50 μL volumes at a final concentration of 500 μM in PBS. H_2O_2 was added in 10-fold excess to a final concentration of 5 mM before incubation at 37 °C for 1 hour. After incubation, the organic products were extracted with 50 μL of ethyl acetate before injection of 5 μL on the GCMS (Shimadzu GCMS-QP5050, RTX5 column: 30 meters, 0.25 mm ID, 0.25 μm film thickness).

4.6. ROS selectivity test

Solutions of **6a-6c** used for HPLC were prepared in 50 μL volumes at a final concentration of 150 μM in PBS. Each ROS was added in a 5–fold excess to a final concentration of 750 μM before incubation at 37 °C for 1 hour. After incubation, the solutions were centrifuged (6000 rpm, 2 min) prior to injection on the HPLC (30 minutes isocratic 50:50 MeOH: H_2O, Kromasil 100-5-C18, 4.6 x 250 mm, 0.5 mL/min, followed at 226 nm). H_2O_2, hypochlorite (NaOCl), and tert-butylhydroperoxide

(TBHP) were delivered from 30%, 70%, and 10% aqueous solutions, respectively. Superoxide ($O_2^{\cdot-}$) was generated from the enzymatic reaction of xanthine oxidase (2 units, 0.5 μL) and hypoxanthine (5 μL of 10 mM stock) in the presence of 5 units of catalase to quench any H_2O_2. Nitric Oxide (NO) was generated from NOC5 (stock solution 1 mM in 0.1 M NaOH); degradation of 1050 μM NOC5 in aqueous solution will generate 750 μM after 60 min. Hydroxyl Radical ($OH^{\cdot}$) was generated by mixing 25 μL of 30 mM H_2O_2 with 25 μL of 150 mM Fe^{2+}.

4.7. Luciferase assay

The transcriptional activation of the ligands were assessed using the Human Estrogen Receptor Beta reporter assay system (Indigo Biosciences). ERβ reporter cells consisting of an ERβ-responsive promoter gene linked to the luciferase gene were defrosted and seeded into a 96-well plate. The cells were treated with the ligands at the indicated concentrations according to the manufacturer's protocol. After 24 hours of incubation, the treatment media was discarded and the luciferase detection reagent added. The luminescence of each sample well was quantified using a SpectraMax i3 plate reader after 10 minutes of incubation at room temperature.

Acknowledgments

This work was supported by start-up funds from the University of Richmond (J.A.P.). H.P. and J.D.M. were recipients of Puryear-Topham-Pierce fellowships from the chemistry department at the University of Richmond and acknowledge support from the University of Richmond Arts and Sciences Undergraduate Research Committee. The authors would like to thank Prof. Michelle Hamm and Dr. Diane Kellogg for their help with instrumentation and Phil Joseph and Robert Plymale who are essential to the success of the undergraduate research program at the University of Richmond.

References and notes

1. Glass, C.K.; Saijo, K.; Winner, B.; Marchetto, M.C.; Gage, F.H. *Cell* **2010**, *140,* 918-934.
2. Uttara, B.; Singh, A.V.; Zamboni, P.; Mahajan, R.T. *Curr. Neuropharmacol*. **2009**, *7*, 65-74.
3. Straub, R.H. *Endocrine Rev.* **2007**, *28*, 521-574.
4. Kuivila, H.G.; Armour, A.G. *J. Am. Chem. Soc.* **1957**, *79*, 5659-5662.
5. Albers, A.E.; Okreglak, V.S.; Chang, C.J. *J. Am. Chem. Soc.* **2006**, *128,* 9640-9641.
6. Major Jourden, J.L.; Cohen, S.M. *Angew. Chem. Int. Ed. Engl.* **2010**, *49*, 6795-6797.
7. Charkoudian, L.K.; Pham, D.M.; Franz, K.J. *J. Am. Chem. Soc.* **2006**, *128*, 12424-12425.
8. Franks, A.T.; Franz, K.J. *Chem. Comm.* **2014**, *50*, 11317-11320.
9. Chen, W.; Balakrishnan, K.; Kuang, Y.; Han, Y.; Fu, M.; Gandhi, V.; Peng, X. *J. Med. Chem.* **2014**, *57*, 4498-4510.
10. Kuang, Y.; Balakrishnan, K.; Gandhi, V.; Peng, X. *J. Am. Chem. Soc*. **2011**, *133*, 19278-19281.
11. Vadukoot, A.K.; AbdulSalam, S.F.; Wunderlich, M.; Pullen, E.D.; Landero-Figueroa, J.; Mulloy, J.C.; Merino, E.J. *Bioorg. Med. Chem Lett.* **2014**, *22*, 6885-6892.
12. Liao, Y.; Xu, L.; Ou, S.; Edwards, H.; Luedtke, D.; Ge, Y.; Qin, Z. *ACS Med. Chem. Lett.* **2018**, *9*, 635-640.
13. Jiang, Q.; Zhong, Q.; Zhang, Q.; Zheng, S.; Wang, G. *ACS Med. Chem. Lett.* **2012**, 3, 392-396.
14. Zhang, C.; Zhong, Q.; Zhang, Q.; Zheng, S.; Miele, L.; Wang, G. *Breast Cancer Res. Treat.* **2015**, *152*, 283-291.
15. Zhong, Q.; Zhang, C.; Zhang, Q.; Miele, L.; Zheng, S.; Wang, G. *BMC Cancer*, **2015**, *15,* 625.
16. Meyers, M.J.; Sun, J.; Carlson, K.E.; Marriner, G.A.; Katzenellenbogen, B.S.; Katzenellenbogen, J.A. *J. Med. Chem.*, **2001**, *44,* 4230-4251.
17. Carroll, V.M.; Jeyakumar, M.; Carlson, K.E.; Katzenellenbogen, J.A. *J. Med. Chem.* **2012**, *55*, 528-537.
18. Brown, C.M.; Mulcahey, T.A.; Filipek, N.C.; Wise, P.M. *Endocrinol.* **2010**, *151*, 4916-4925.
19. Crawford, D.K.; Mangiardi, M.; Song, B.; Patel, R.; Du, S.; Sofroniew, M.V.; Voskuhl, R.R.; Tiwari-Woodruff, S.K. *Brain* **2010**, *133*, 2999-3016.
20. Kumar, S.; Patel, R.; Moore, S.; Crawford, D.K.; Suwanna, N.; Mangiardi, M.; Tiwari-Woodruff, S.K. *Neurobiol. Dis.* **2013**, *56*, 131-144.
21. Lewis, D.K.; Johnson, A.B.; Stohlgren, S.; Harms, A.; Sohrabji, F. *J. Neuroimmunol.* **2008**, *195*, 47-59.
22. Saijo, K.; Collier, J.G.; Li, A.C.; Katzenellenbogen, J.A.; Glass, C.K. *Cell* **2011**, *145*, 584-595.
23. Smith, J.A.; Das, A.; Butler, J.T.; Ray, S.K.; Banik, N.L. *Neurochem. Res.* **2011**, *36*, 1587-1593.
24. Suwanna, N.; Thangnipon, W.; Kumar, S.; de Vellis, J. *EXCLI J.* **2014**, *13*, 1097-1103.
25. Yu, H.P.; Hsieh, Y.C.; Suzuki, T.; Shimizu, T.; Choudhry, M.A.; Schwacha, M.G.; Chaudry, I.H. *Am. J. Physiol. Lung Cell Mol. Physiol.* **2006**, *290*, L1004-1009.
26. Mohler, M.L.; Narayanan, R.; Coss, C.C.; Hu, K.; He, Y.; Wu, Z.; Hong. S.S.; Hwang, D.J.; Miller, D.D.; Dalton, J.T. *Expert Opin. Ther. Pat.* **2010**, *20*, 507-534.
27. Paterni, I.; Granchi, C.; Katzenellenbogen, J.A.; Minutolo, F. *Steroids* **2014**, *90*, 13-29.
28. Farooq, A. *Curr. Top. Med. Chem.* **2015**, *15*, 1372-1384.
29. Pike, A.C.W.; Brzozowski, A.M.; Hubbard, R.E.; Walton, J.; Bonn, T.; Thorsell, A.-G.; Engstrom, O.; Ljunggren, J.; Gustaffson, J.-A.; Cariquist, M. PDB: 2J7X
30. Manas, E.S.; Xu, Z.B.; Unwalla, R.J.; Somers, W.S. *Structure*, **2004**, *12*, 2197-2207.
31. Govan, J.M.; McIver, A.L.; Riggsbee, C.; Deiters, A. *Angew. Chem. Int. Ed. Engl.* **2012**, *51*, 9066-9070.
32. Carlson, K.E.; Choi, I.; Gee, A.; Katzenellenbogen, B.S.; Katzenellenbogen, J.A. *Biochemistry* **1997**, *36,* 14897-14905.
33. Blair, R.M.; Fang, H.; Branham, W.S.; Hass, B.S.; Dial, S.L.; Moland, C.L.; Tong, W.; Shi, L.; Perkins, R.; Sheehan, D.M. *Toxicol. Sci.* **2000**, *54*, 138-153.
34. Sikora, A.; Zielonka, J.; Lopez, M.; Joseph, J.; Kalyanaraman, B. *Free Rad. Biol. Med.* **2009**, *47*, 1401-1407.
35. Sun, X.; Xu, Q.; Kim, G.; Flower, S.E.; Lowe, J.P.; Yoon, J.; Fossey, J.S.; Qian, X.; Bull, S.D.; James, T.D. *Chem. Sci.* **2014**, *5*, 3368-3373.
36. Wyatt, A.R.; Kumita, J.R.; Mifsud, R.W.; Gooden, C.A.; Wilson, M.R.; Dobson, C.M. *Proc. Nat. Ac. Sci.* **2014**, *111*, E2081-E2090.
37. Coombes, E.; Jiang, J.; Chu, X.-P.; Inoue, K.; Seeds, J.; Branigan, D.; Simon, R.P.; Xiong, Z.-G. *Antioxid. Redox Signal.* **2011**, *14*, 1815-1827.
38. Mayes, J.; Tinker-Mill, C.; Kolosov, O.; Zhang, H.; Tabner, B.J.; Allsop, D. *J. Biol. Chem*. **2014**, *289*, 12052-12062.
39. Yang, J.; Yang, J.; Liang, S.G.; Xu, Y.; Moore, A.; Ran, C. *Sci. Rep.* **2016**, *6*, 35613.
40. Grosdidier, A.; Zoete, V.; Michielin, O. *Nucleic Acids Res.* **2011**, *39,* W270-277.
41. Grosdidier, A.; Zoete, V.; Michielin, O. *J. Comput. Chem.* **2011**, *32*, 2149-2159.
42. Humphrey, W.; Dalke, A.; Schulten, K. *J. Molec. Graphics*, **1996**, *14*, 33-38.

Supplementary Material

Supplementary data associated with this article can be found in the online version.